

---

---

# Potential of PET to Predict the Response to Trastuzumab Treatment in an ErbB2-Positive Human Xenograft Tumor Model

Gabriela Kramer-Marek\*<sup>1</sup>, Merel Gijssen\*<sup>2</sup>, Dale O. Kiesewetter<sup>3</sup>, Ruth Bennett<sup>2</sup>, Ioannis Roxanis<sup>4</sup>, Rafal Zielinski<sup>1</sup>, Anthony Kong<sup>2</sup>, and Jacek Capala<sup>1</sup>

<sup>1</sup>Radiation Oncology Branch, Center for Cancer Research, National Cancer Institute, Bethesda, Maryland; <sup>2</sup>Weatherall Institute of Molecular Medicine, University of Oxford, Oxford, United Kingdom; <sup>3</sup>National Institute of Biomedical Imaging and Bioengineering, NIH, Bethesda, Maryland; and <sup>4</sup>Department of Cellular Pathology, Oxford University Hospitals and Oxford Biomedical Research Centre, Oxford, United Kingdom

Currently, an alteration in the gross volume of a tumor is used to assess its response to trastuzumab; however, this approach provides only a late indication of response. Tissue-sample ex vivo assays are potentially valuable, but their procurement through biopsies is invasive and might be biased by tumor heterogeneity. We studied the feasibility of using PET to quantify changes in ErbB2 (*HER2/neu*) expression and to predict the response to trastuzumab in BT474 breast cancer xenografts with *N*-[2-(4-<sup>18</sup>F-fluorobenzamido)ethyl]maleimide (<sup>18</sup>F-FBEM)-HER<sub>2:342</sub> Affibody. **Methods:** Mice bearing BT474 tumors were given trastuzumab (50 mg/kg loading dose, 25 mg/kg maintenance dose, administered intraperitoneally twice a week) or saline (control) for a total of 5 doses. Tumor size was monitored twice a week. Animals were scanned before the treatment, at 48 h, and 2 wk after the beginning of therapy. After the final scan, PET results were correlated with tumor response and immunohistochemical assessment of ErbB2 level, as well as with vasculature in the treated tumors. **Results:** Analysis of PET images indicated that tracer uptake was significantly reduced after 1 dose of trastuzumab, compared with baseline, suggesting applicability as an early indicator of changes in ErbB2 expression. After 5 doses of trastuzumab, the overall decrease in <sup>18</sup>F-FBEM-HER<sub>2:342</sub> Affibody uptake also correlated with tumor response and downregulation of ErbB2 expression by immunohistochemical assessment. However, individual animals had different responses. There was a correlation between bigger PET changes and a higher vessel count in the tumors, suggesting that an increased number of vessels could lead to better trastuzumab delivery. We confirmed that the difference in average vessel count in the tumors was not related to the size of the tumors and therefore was not due to the selection of more vascular tumors. This finding is consistent with previous findings demonstrating that the number of vessels in a tumor could be a useful prognostic marker for treatment response. **Conclusion:** Our data suggest

that Affibody-based PET can noninvasively provide specific information on changes in receptor expression and could be a valuable strategy for predicting tumor response to trastuzumab.

**Key Words:** breast cancer HER2/ErbB2; trastuzumab; PET imaging; Affibody molecules

**J Nucl Med 2012; 53:629–637**

DOI: 10.2967/jnumed.111.096685

**T**he transmembrane receptor ErbB2 (*HER2/neu*) belongs to the epidermal growth factor receptor family of tyrosine kinases. It induces signaling pathways that promote a wide range of cellular processes, including proliferation, differentiation, survival, angiogenesis, and antiapoptotic functions (1). The amplification and overexpression of ErbB2 occur in 18%–25% of human breast cancers, depending on the diagnostic technique used, and are predictive of more aggressive disease and a poor clinical outcome (2,3). Numerous efforts have taken place to develop ErbB2-targeted therapies (4); however, the only one approved by the Food and Drug Administration for primary treatment is trastuzumab (Herceptin; Genentech, Inc.), a recombinant humanized anti-ErbB2 monoclonal antibody that specifically binds to the juxtamembrane portion of the extracellular domain of ErbB2. Trastuzumab has been shown to downregulate ErbB2 receptors both in vitro and in vivo (5,6), although it does not decrease ErbB2 phosphorylation (7). In animal models, the activity of trastuzumab was found to depend on the engagement of natural killer cells, identifying antibody-dependent cellular cytotoxicity as the major mechanism of trastuzumab action (8,9). Additional mechanisms of trastuzumab may include suppression of angiogenesis by modulating the effects of different pro- and antiangiogenic factors (10).

In clinical studies, trastuzumab apparently improves survival when given concomitantly or sequentially with chemotherapy (11,12). Its efficacy as a single agent has not met expectations (13), and less than 30% of patients with

Received Aug. 15, 2011; revision accepted Dec. 16, 2011.

For correspondence or reprints contact either of the following:

Jacek Capala, National Cancer Institute, NIH, 6130 Executive Blvd., Room 6010, Rockville, MD 20852-7440.

E-mail: capalaj@mail.nih.gov

Anthony Kong, Weatherall Institute of Molecular Medicine, University of Oxford, John Radcliffe Hospital, Oxford OX3 9DS, U.K.

E-mail: anthony.kong@imm.ox.ac.uk

\*Contributed equally to this work.

Published online Mar. 12, 2012.

COPYRIGHT © 2012 by the Society of Nuclear Medicine, Inc.

ErbB2-overexpressing metastatic breast cancer respond to first-line trastuzumab therapy (14). Moreover, most of the initial responders eventually acquired resistance to trastuzumab (13,14). Because high levels of ErbB2 may predict response to trastuzumab (15), the clinical efficacy of trastuzumab as a molecularly targeted therapy may depend on the precise assessment of ErbB2 status. Currently, the only reliable method to evaluate the response to trastuzumab is to assess tumor size through conventional radiologic measurements of changes in gross tumor volume, which tend to be a late indicator of response. It is possible, though, that altering ErbB2 expression with trastuzumab might provide an early indication of response. To assess ErbB2 status before and after trastuzumab treatment, *ex vivo* methods including immunohistochemical staining for protein overexpression and probing for ErbB2 gene amplification by fluorescence *in situ* hybridization are potentially valuable. However, procuring tumor tissues through biopsies to evaluate drug action is invasive, and reliable results are limited by sample bias stemming from tumor heterogeneity and other confounding factors such as inflammation. Because obtaining serial biopsy material to assess the effects of therapy is clinically impractical, there is an urgent need to effectively and accurately measure ErbB2 expression level before and during the treatment, possibly using a non-invasive molecular technique.

*In vivo* evaluation of ErbB2 expression level using PET might provide a valuable strategy for predicting tumor response to trastuzumab in real time. If verified, such information could allow for dosing schedule optimization for individual patients and identify nonresponders who could be offered an alternative therapy, thereby improving the treatment outcome and sparing unnecessary costs. Moreover, such information could also help to prevent false-positive or false-negative scores due to the heterogeneity of receptor expression in biopsy probes. Although multiple phase I clinical trials with radiolabeled trastuzumab are ongoing, the intact antibodies, appropriate for therapeutic strategies, are not optimal for imaging (16,17). Finally, using labeled trastuzumab to monitor changes in ErbB2 levels after therapy with the drug itself might introduce a systematic error due to competition for binding to the receptor.

Therefore, in this work, we are taking advantage of the fact that our tracer and trastuzumab bind to distinct epitopes on the ErbB2 extracellular domain (18), by investigating the effect of trastuzumab on ErbB2 expression in a preclinical breast cancer xenograft model. We correlate PET results with tumor response and immunohistochemical assessment of ErbB2 level and with vasculature in the treated tumors.

## MATERIALS AND METHODS

### Cell Line and Reagents

Tumor breast carcinoma BT474 with highly overexpressing ErbB2 (19) was obtained from the American Type Culture Collection. The cells were cultured in RPMI 1640 medium supplemented with 10% (v/v) heat-inactivated fetal bovine serum (Gibco) and

penicillin/streptomycin (a 100-U/mL concentration of each). Cells were grown as a monolayer at 37°C in a humidified atmosphere containing 5% CO<sub>2</sub>.

The Z<sub>HER2:342</sub>-Cys Affibody molecules were kindly provided by our Cooperative Research and Development Agreement partner in Sweden (Affibody AB). <sup>18</sup>F-radiolabeled was produced via the <sup>18</sup>O (p,n)<sup>18</sup>F nuclear reaction at the cyclotron facility of the Clinical Center at the National Institutes of Health by irradiating <sup>18</sup>O-enriched water. N-[2-(4-<sup>18</sup>F-fluorobenzamido)ethyl]maleimide (<sup>18</sup>F-FBEM)-HER<sub>2:342</sub> Affibody was prepared as previously described (20).

### Animal Experiments

This study was approved by the Animal Care and Use Committee of the National Institutes of Health and performed in accordance with the Department of Health and Human Services' *Guide for the Care and Use of Laboratory Animals*. Female athymic nude mice were implanted with 0.72-mg 90-d-release 17β-estradiol pellets (Innovative Research) 1 d before cell inoculation. BT474 cells (6 × 10<sup>6</sup>) in a 100-μL mixture of phosphate-buffered saline and Matrigel (0.7:0.3 ratio; BD Bioscience) were injected subcutaneously into the right back shoulder. The mean tumor volume before treatment initiation for all animals was 100–200 mm<sup>3</sup>. The control and treatment groups consisted of 6–8 mice each. In total at the end of the study, there were 18 control and 24 treated animals. Trastuzumab (50 mg/kg loading dose, 25 mg/kg maintenance dose) was given intraperitoneally twice a week for 2 wk. At the same time, the control animals were injected with a saline vehicle (0.2 mL, intraperitoneally). Using caliper measurements (volume = length × width<sup>2</sup>/2), the tumor size was monitored twice a week. Percentage change in tumor volume from baseline was calculated according to the following formula:

$$\% \Delta_{\text{volume}} = 100 \times \frac{\text{Vol}_{t=x} - \text{Vol}_{t=0}}{\text{Vol}_{t=0}}$$

### PET

PET scans were obtained for each animal before treatment, after the initial dose, and at the end of treatment using the National Institutes of Health Advanced Technology Laboratory Animal Scanner. The mice were anesthetized using isoflurane/O<sub>2</sub> (1.5%–2.0% v/v), placed prone in the center of the field of view of the scanner, and given an injection of <sup>18</sup>F-FBEM-HER<sub>2:342</sub> Affibody (3.7–6.7 MBq, 10–13 μg, 100 μL) via the lateral tail vein. A 10-min emission scan (single field of view) was recorded 1 h after injection with a 100- to 700-keV energy window. The images were reconstructed with a 2-dimensional ordered-subsets expectation maximization algorithm. No correction was applied for attenuation or scatter. For each scan, regions of interest were manually drawn over the tumor and normal tissue. The maximum counts per pixel within the tumor or normal tissues were obtained from multiple regions of interest (counts/s/cm<sup>3</sup>). The results were calculated as percentage injected dose per gram using a calibration constant obtained from scanning the <sup>18</sup>F source, assuming a tissue density of 1 g/mL, and dividing by the injected dose, which was decay-corrected to the time of scanning.

### Histopathology

Following the final PET acquisition after the single and fifth doses of trastuzumab, randomly selected mice were sacrificed by cervical dislocation. Histopathology was performed to confirm the presence of neoplastic cells, determine the presence of ErbB2 receptors, and analyze the tumor vasculature. Tumors were excised, frozen in

liquid nitrogen and stored at  $-80^{\circ}\text{C}$  or fixed with 10% neutral buffered formalin solution. Frozen or paraffin-embedded tissue specimens from control and treated mice were sectioned, and 4- $\mu\text{m}$ -thick sections were stained with hematoxylin and eosin, as well as rabbit anti-human ErbB2 (Cell Signaling) and rat anti-murine CD31 (Dianova) antibodies. The specimens were freed of wax and rehydrated before antigen retrieval was performed. For ErbB2 staining, Tris/ethylenediamine tetraacetic acid, pH 9, was used for antigen retrieval. Sections were incubated overnight with primary antibodies at  $4^{\circ}\text{C}$  and the next day with a peroxidase-coupled antirabbit secondary antibody (Vector Laboratories) for half an hour at room temperature. A diaminobenzidine peroxidase substrate (Vector Laboratories) was used to visualize staining. For the combined ErbB2 and CD31 staining, citrate buffer, pH 6, was used to retrieve the antigen. Sections were incubated with ErbB2 antibody for 1 h at room temperature. Next, a peroxidase-coupled antirabbit secondary antibody was incubated with the sections for half an hour. A diaminobenzidine peroxidase substrate was used to visualize staining. The same section was then incubated with the CD31 antibody for 1 h at room temperature. A peroxidase-coupled antirat secondary antibody (Vector Laboratories) was incubated for half an hour before a SG peroxidase substrate (Vector Laboratories) was used according to the manufacturer's instructions. Sections were counterstained using nuclear fast red (DAKO) and dehydrated before using a permanent mount (Vectamount) to mount the sections. Sections were washed in phosphate-buffered saline between all staining steps.

The slides were analyzed and scored for intensity (0, 1, 2, or 3), as well as for the percentage of this intensity (0%–100%) that could be found in the section. The intensity percentage score (IPS) was then calculated by multiplying the percentage and intensity (e.g.,  $2 \times 20\%$ ), and at the end, all intensities were added together (e.g.,  $1 \times 30\% + 2 \times 20\% + 3 \times 50\% = 220$  IPS).

To determine the amount of vessels in a tumor sample, after immunohistochemical costaining of ErbB2 and CD31, 10 random views were selected from both the center and the periphery of the tumor slide. The number of vessels in each view was counted and averaged over the 10 views. We plotted the number of vessels against PET tracer uptake and IPS scoring of ErbB2.

### Western Immunoblot Analysis

Frozen tumor tissues collected from randomly selected animals (3 controls, 6 treated) after a single dose of trastuzumab were weighed and sliced into small pieces. Afterward, the specimens were placed in a lysis buffer containing protease and phosphate inhibitors and were homogenized on ice, using a Polytron homogenizer. Cell debris was removed through centrifugation of the suspensions at 13,000 rpm ( $4^{\circ}\text{C}$ ) for 15 min. The supernatants were collected and stored at  $-80^{\circ}\text{C}$ . Before use, the protein concentration was determined using the bicinchoninic acid protein kit assay (Pierce) according to the manufacturer's protocol. Total cellular proteins (30–60  $\mu\text{g}$ ) were resolved on 4%–12% NuPAGE Novex tris-acetate gel (Invitrogen) by electrophoresis and transferred to a nitrocellulose membrane, which was subsequently blocked for 1 h at room temperature with 5% nonfat milk-blocking buffer. All reagents for NuPAGE and Western blots were from Invitrogen. Thereafter, proteins were immunoblotted with a polyclonal antibody against ErbB2 (Cell Signaling Technology) or a loading control—the mouse monoclonal antibody anti- $\beta$ -actin (GenWay Biotech, Inc.)—at  $4^{\circ}\text{C}$  overnight. After extensive rinsing with a washing buffer (Tris-buffered saline, polysorbate),

membranes were incubated with the secondary antibodies—horse-radish peroxidase-conjugated goat antirabbit and antimouse IgG<sub>1</sub>—for 1 h at room temperature. After final washing, immunoblots were visualized with a chemiluminescence detection system (Pierce) and an LAS-4000 Luminescent Image Analyzer (Fujifilm). Data were analyzed with Multi Gauge (version 3.0; Fujifilm) software.

### Statistical Analysis

Tumor uptake of  $^{18}\text{F}$ -FBEM-HER<sub>2:342</sub> Affibody was compared between control and trastuzumab-treated mice using the nonparametric, 2-tailed Mann–Whitney test. The same test was used to evaluate the relationship between changes in tumor volume and 3 PET groups. The differences between groups were considered statistically significant when the *P* values were less than 0.05. Median and 95% confidence intervals were reported. Changes in the PET signal versus tumor volume were tested for an association using the Pearson correlation test, which takes advantage of the continuous nature of the variables. All data were analyzed using Prism5 (GraphPad Software).

## RESULTS

We investigated the efficacy of trastuzumab (50 mg/kg loading dose, followed by 4 additional doses of 25 mg/kg) during the 2-wk treatment course in mice bearing BT474 tumor xenografts. Tumor-bearing mice were injected with  $^{18}\text{F}$ -FBEM-HER<sub>2:342</sub> Affibody or saline and scanned by small-animal PET 3 times: before the first dose, 48 h after receiving the loading dose, and at the end of the trastuzumab treatment. Each time, the tracer accumulation was quantified and the results were normalized to baseline.

### PET Analysis, but Not Immunohistochemical Staining or Western Blot, Revealed Reduced Level of ErbB2 After Single Dose of Trastuzumab

Figure 1 shows representative PET coronal sections before treatment, after the single dose, and after the final dose. The images obtained after 1 dose of trastuzumab clearly indicate a decrease in radiotracer uptake, compared with baseline, most likely resulting from a decrease in the ErbB2 level. We found a 20% statistically significant reduction of  $^{18}\text{F}$ -FBEM-HER<sub>2:342</sub> Affibody uptake in the treated mice, compared with the control (Fig. 2A, *P* < 0.0001). Treatment with saline solution alone did not alter the tracer accumulation.

To confirm that the decrease in tracer uptake was due to the decrease in the ErbB2 level, we performed *ex vivo* analysis of randomly selected tissue samples (control, *n* = 3; treated, *n* = 6). The immunohistochemical staining of ErbB2 membrane expression did show variability between analyzed tissue samples. Stratifying the expression pattern using discrete regions revealed a significant level of ErbB2 heterogeneity within the individual sections (Fig. 2B). Consequently, some areas were assessed as 3+ and 1+ within the tumor tissue sample. Some trastuzumab-treated tumors showed clear ErbB2 downregulation (Fig. 2B, right panel), whereas some showed only a minimal reduction in ErbB2 expression on the cell surface (Fig. 2B, left panel). Quantification of the membrane staining using the IPS scoring system (“Materials and Methods”) indicated no significant

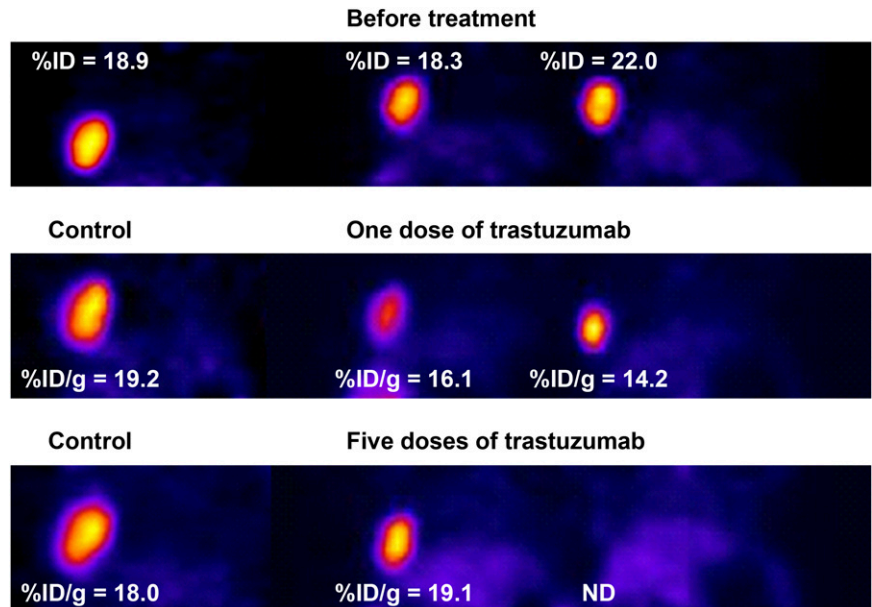


**FIGURE 1.** Representative coronal sections acquired 1 h after tracer injection in 3 mice bearing BT474 tumors. Images were collected before treatment (top), after initial single dose of trastuzumab (middle), and after additional 4 doses of trastuzumab (bottom). There were significant changes in  $^{18}\text{F}$ -FBEM-HER<sub>2:342</sub> Affibody accumulation after initial dose of trastuzumab, whereas after 2 wk of treatment some mice showed complete remission (right mouse at bottom) and some mice with nonresponsive tumors did not show any decrease in tracer uptake from baseline (middle).

difference between the control and treated groups (Fig. 2C). This heterogeneity was probably the reason why the IPS scoring did not correspond to PET analysis. Interestingly, Western blot analysis of the ErbB2 expression level did not detect those changes in tissue lysates from the same tumors (Fig. 2D).

**Five Doses of Trastuzumab Caused Overall Reduction in Tracer Uptake and Tumor Growth Inhibition Despite Heterogeneity**

After 2 wk of treatment, we observed a rapid progression of tumors within the control mice, which were receiving only

saline. The mean percentage increase in tumor volume from baseline was  $137\% \pm 21\%$ , and in some cases the increase was as high as 300% in 14 d (Fig. 3A). In the treated group, trastuzumab significantly inhibited tumor growth, compared with control ( $P = 0.0004$ ), resulting in a dramatic tumor regression in 8 of 24 mice (Fig. 3A). In 2 mice, we observed complete tumor remission; therefore, those animals were not included in the final PET analysis.

Although we have shown that trastuzumab significantly inhibited tumor growth, compared with control, analysis of PET images after 5 doses of trastuzumab showed diver-

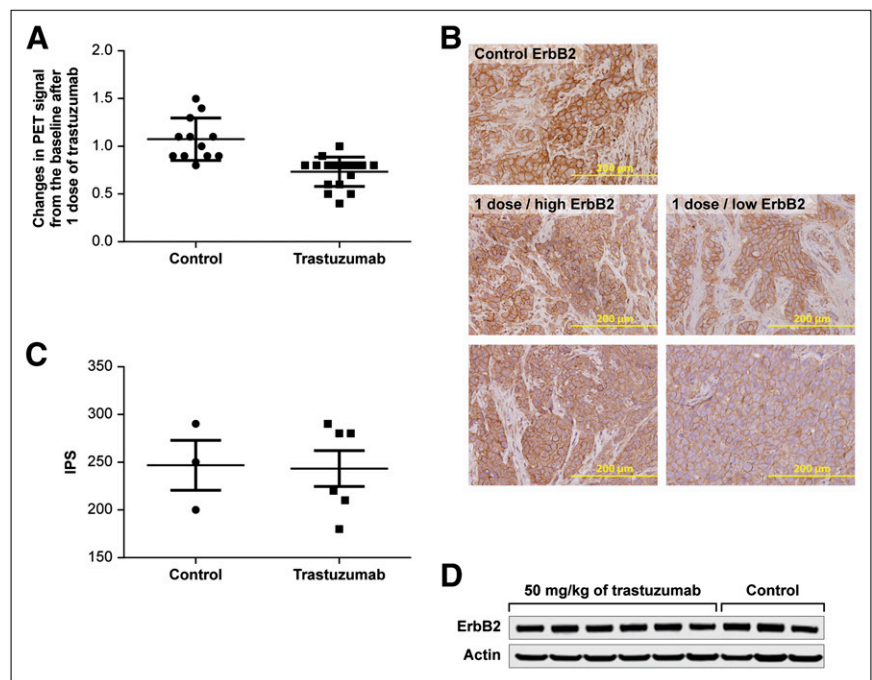


**FIGURE 2.** Changes in ErbB2 expression in mice bearing BT474 tumors and in extracted tumor tissues 48 h after trastuzumab treatment (single dose, 50 mg/kg). (A) Quantified  $^{18}\text{F}$ -FBEM-HER<sub>2:342</sub> Affibody uptake in control and trastuzumab-treated mice normalized to baseline (control vs. trastuzumab  $P < 0.0001$ ). (B) Representative tumor sections from formalin-fixed, paraffin-embedded tumor tissues originated from different animals. Cell surface of ErbB2 was detected with anti-ErbB2 monoclonal antibody that does not cross-react with trastuzumab. (C) IPS scoring, based on immunohistochemical staining for selective animals (control [ $n = 3$ ] vs. trastuzumab [ $n = 6$ ];  $P = 1$ ). (D) Representative Western blots of ErbB2 expression.

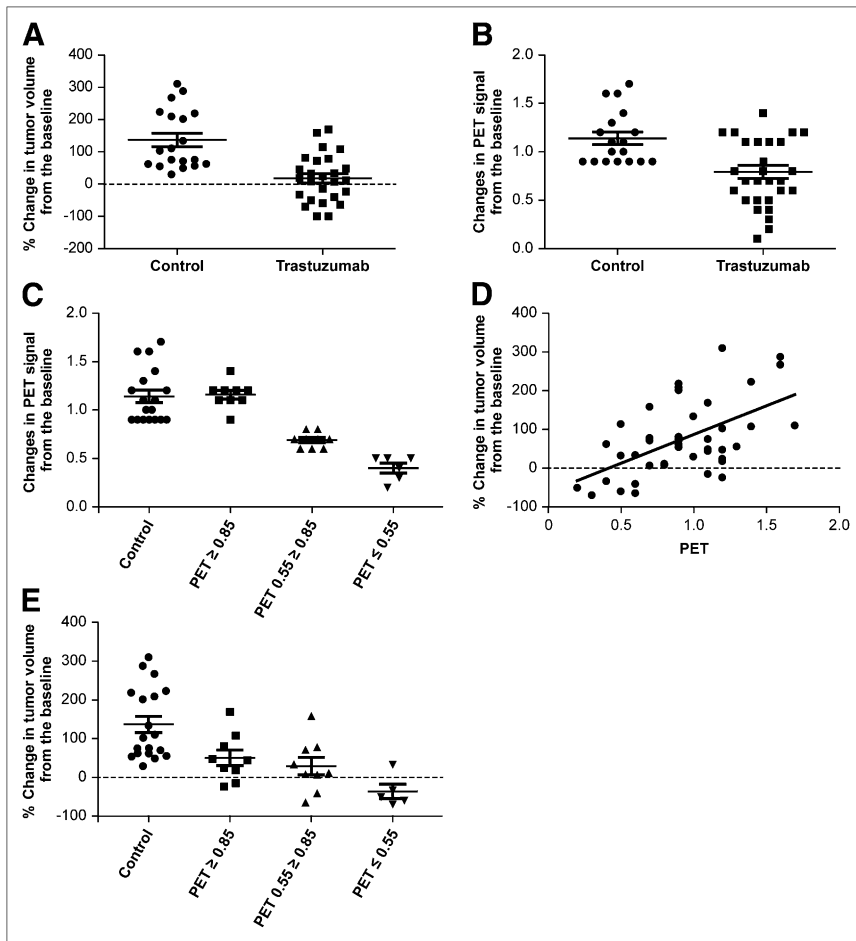


**FIGURE 3.** Mice received 5 doses of drug: 1 loading dose (50 mg/kg) and 4 maintenance doses (25 mg/kg). (A) Percentage changes in tumor volume from baseline in mice treated with control vehicle or with trastuzumab [control ( $n = 19$ ) vs. trastuzumab ( $n = 24$ );  $P = 0.0004$ ]. (B) Quantified  $^{18}\text{F}$ -FBEM-HER $_{2:342}$  Affibody uptake in control and trastuzumab-treated mice normalized to baseline (control vs. trastuzumab;  $P = 0.0007$ ). (C) Trastuzumab-treated mice divided into 3 groups using PET signal changes from baseline according to the following cutoffs:  $\geq 0.85$ ,  $0.55 \leq 0.85$ , and  $\leq 0.55$ . Tracer accumulation showed statistically significant decrease compared with control in 2 groups: control vs.  $0.55 \leq 0.85$ ,  $P = 0.0001$ ; control vs.  $\leq 0.55$ ,  $P = 0.0003$ . For cutoff of  $\geq 0.85$ , there were no significant changes (control vs.  $\geq 0.85$ ,  $P = 0.445$  [Mann-Whitney test]). (D) Changes in PET signal plotted against changes in tumor size. (E) Relationship between changes in tumor volume and 3 PET groups. We found that tumor response and changes in PET signals were positively related (control vs.  $\geq 0.85$ ,  $P = 0.01$ ; control vs.  $0.55 \leq 0.85$ ,  $P = 0.006$ ; control vs.  $\leq 0.55$ ,  $P = 0.0011$  [Mann-Whitney test]).

gence in tumor response (Fig. 3B). Quantification of radio-tracer uptake at the end of the trastuzumab treatment showed that the signal decreased in only some of the mice (Fig. 1, bottom right), whereas only a slight change from baseline was seen in the other mice (Fig. 1, bottom middle).

To account for this finding, the animals were arranged into 3 groups based on the PET signal changes from baseline according to the following cutoffs:  $\geq 0.85$ ,  $0.55 \leq 0.85$ , and  $\leq 0.55$  (Fig. 3C). Analysis of regions of interest drawn around the tumors in the control group indicated no changes in tracer uptake. Also, no significant changes in tracer accumulation were found in 9 of 24 treated tumors (control vs.  $\geq 0.85$ ,  $P = 0.445$ ). In contrast to these data, in 9 of 24 tumors we observed a 55%–80% loss in  $^{18}\text{F}$ -FBEM-HER $_{2:342}$  Affibody uptake (control vs.  $0.55 \leq 0.85$ ,  $P = 0.0001$ ), and furthermore, in 6 of 24 mice, the tumor uptake was less than 50% (control vs.  $\leq 0.55$ ,  $P = 0.0003$ ).

To address the question of whether PET might predict tumor response, we also analyzed the relationship between tracer uptake and changes in tumor volume (Fig. 3D). We showed that PET response correlated positively with the percentage of tumor volume ( $R^2 = 0.30$ ,  $P = 0.0001$ ). Notably, we found that tumor response measured by tumor size also correlated with PET signals according to the fol-

lowing PET cutoffs:  $\geq 0.85$ ,  $P = 0.01$ ;  $0.55 \leq 0.85$ ,  $P = 0.006$ ;  $\leq 0.55$ ,  $P = 0.0011$  (Fig. 3E).

To confirm those findings, selected tumors from each group were analyzed by immunohistochemical staining to assess ex vivo ErbB2 membrane level. In accordance with the observations seen in PET images, we discovered much heterogeneity in receptor expression between individual samples (Fig. 4A). Even though we observed a drop in ErbB2 membrane level in trastuzumab-treated samples versus controls (Fig. 4B), which validated PET in assessing ErbB2 expression in breast tumors, there was also a large overlap between the treated group and the controls.

Separating the treated samples according to the PET cutoffs, we found, surprisingly, that the 50% decrease in tracer uptake was not associated with a similar decrease in ErbB2 level (Supplemental Fig. 1 [supplemental materials are available online only at <http://jnm.snmjournals.org>]). This finding was likely caused by the low numbers in each PET cutoff group that was subjected to ex vivo analysis ( $n = 5$  for  $<0.55$ ) and the fact that the IPS scoring was not sensitive enough to detect changes in differences in intensity for some tumors. There was also a correlation between tumor size and IPS scoring ( $R^2 = 0.35$ ,  $P = 0.0001$ , Fig. 4C), similar to the finding between PET and tumor size (Fig. 3D,  $R^2 = 0.30$ ,  $P = 0.0001$ ).

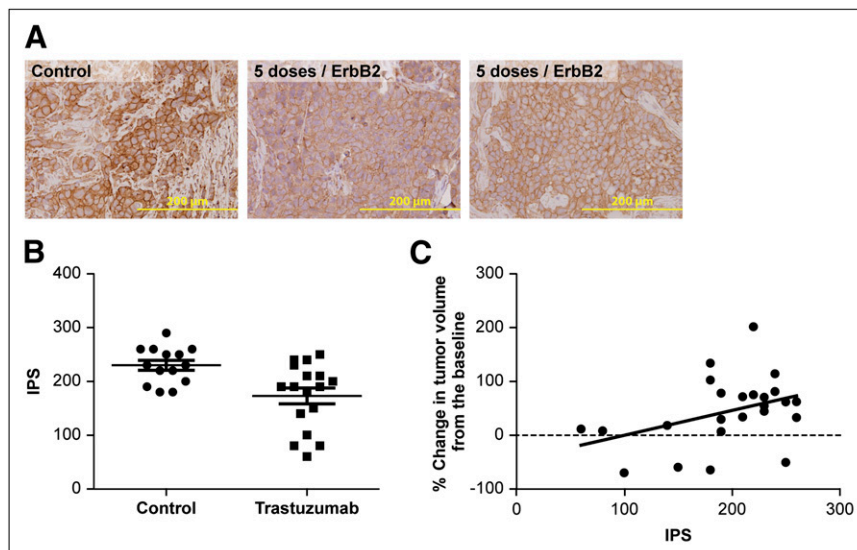


**FIGURE 4.** Immunohistochemical analysis of ErbB2 level on tumor cell surface after treatment with 5 doses of trastuzumab. (A) Photos taken from xenograft samples stained for ErbB2. Left panel shows control xenograft samples, middle and right panels are trastuzumab-treated samples. (B) Quantification of ErbB2 membrane staining by IPS (control,  $n = 14$ ; treated,  $n = 16$ ). (C) Correlation between tumor size and IPS scoring for control mice and mice treated with trastuzumab ( $R^2 = 0.35$ ,  $P = 0.0001$ ,  $n = 24$ ).

Comparison of early changes in Affibody uptake to later tumor response (changes in volume) and changes in PET signal did not provide conclusive results. Although there was a clear trend, the correlation was not significant and graphing it would not provide any additional information.

#### Samples with Lowest PET Signal Had Higher Average Vessel Count

We want to stress that all the mice were from the same strain and that the xenografts originated from the same cell line and were treated the same way, even though the response to trastuzumab treatment was highly diverse. In an attempt to understand the mechanisms responsible for this phenomenon, we hypothesized that tumors with more vessels would show a better response to trastuzumab treatment because of better drug delivery; therefore, we evaluated the variations within the vasculature of the tumors. We stained the vessels with an antibody against endothelial marker CD31 (Fig. 5A) and counted the number of vessels in 10 randomly picked fields within 1 sample. Plotting the average vessel count against the PET changes showed bigger PET changes in samples with a higher vessel count (Fig. 5B). Interestingly, separating the groups according to PET cutoffs revealed a significantly higher average number of vessels in the group of mice with more than 50% lower  $^{18}\text{F}$ -FBEM-HER<sub>2:342</sub> Affibody uptake (Fig. 5C;  $P = 0.02$ ). The non-linear regression analysis also showed a downward trend between the number of vessels and IPS scores of ErbB2—a trend that was more marked in trastuzumab-treated samples (Fig. 5D, bottom) than in controls (Fig. 5D, top) ( $R^2 = 0.12$ ,  $P < 0.0001$ ; Fig. 5D). To confirm that the difference in average vessel count in our samples was not due to the size of the tumor, we plotted the tumor volume and vessel count against each other (Fig. 5E). The results showed that tumor size was not related to average vessel count per field ( $R^2 = 0.0007$ ,  $P = 0.9$ ). Together, these data strongly suggest that

a decrease in the ErbB2 level observed in samples with higher vessel counts most likely occurred because of better trastuzumab delivery, in comparison to the rest of the treated animals.

#### DISCUSSION

In current clinical practice, the assessment of therapeutic efficacy in tumors is based on changes in tumor size; however, even tumors that shrink may contain viable malignancy. Conversely, an apparently unchanged residual mass may represent a posttherapy response, such as inflammation, fibrosis, or necrosis, but not viable cells. Additionally, in some cases when tumor size increases, it is important to know whether the lack of response is due to therapeutic resistance or inadequate drug delivery. Therefore, because molecular alterations precede volumetric changes, PET of tumor biomarkers might provide a means for a more sensitive and specific measure of tumor response.

In the era of targeted therapies, accurate assessment of receptor status plays a pivotal role in the clinical management of breast cancer patients. We have previously demonstrated that PET using the avid binding of  $^{18}\text{F}$ -FBEM-HER<sub>2:342</sub> Affibody to ErbB2 may be applied to quantify changes in ErbB2 expression in breast cancer xenografts treated with 17-DMAG, an Hsp90 inhibitor (19).

In this study, we investigated the defensibility of using PET to monitor changes in ErbB2 expression and whether these changes can be used to predict the response of BT474 xenografts in a 2-wk treatment with trastuzumab. To demonstrate PET sensitivity and specificity, we correlated the imaging results with an overall decrease in tumor size and routinely used ex vivo methods such as immunohistochemical staining and Western blots.

Our data clearly indicate that  $^{18}\text{F}$ -FBEM-HER<sub>2:342</sub> Affibody uptake measured by region-of-interest analysis was



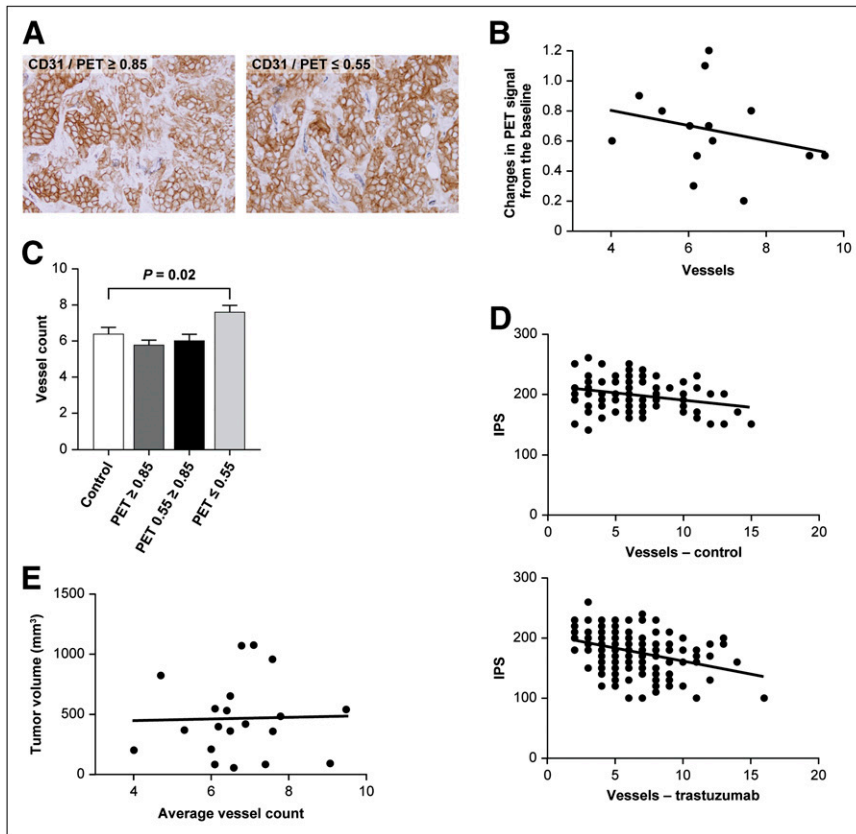


**FIGURE 5.** Analysis of tumor vasculature based on CD31 staining. After CD31 and ErbB2 immunohistochemical costaining, 10 random views from center and periphery of tumor slides were obtained. Number of vessels was scored and averaged over 10 views. (A) Two representative examples of tumor slides from trastuzumab-treated mice: PET cutoffs of  $\geq 0.85$  (left panel) and  $\leq 0.55$  (right panel). (B) Average vessel count per field in a trastuzumab-treated xenograft sample plotted against PET changes observed for the same xenograft ( $n = 14$ ). (C) Average number of vessels in control group ( $n = 6$ ) and trastuzumab-treated group ( $n = 14$ ) with various PET cutoffs. (D) Correlation between IPS scoring and number of vessels in control group ( $n = 6$ , 10 fields for each) and trastuzumab-treated groups ( $n = 14$ , 10 fields for each). (E) Tumor size plotted against average vessel count per field (control,  $n = 6$ ; treated,  $n = 14$ ).

significantly reduced ( $P = 0.0001$ ) after just 1 dose of trastuzumab, compared with baseline, suggesting its applicability as an early indicator of changes in ErbB2 expression. Surprisingly, this decrease in ErbB2 was not detected by Western blot, most likely because this technique analyzes all the cellular compartments of tumor cells and is not sensitive enough to pick up subtle differences in ErbB2 membrane levels. The overall immunohistochemical scoring of neither the treated tumor samples nor the control indicated a statistically significant reduction in ErbB2 expression, which might be attributed to tumor heterogeneity and low sensitivity of the immunohistochemical scoring system in detecting small differences in staining intensity after 1 dose of trastuzumab. Also, the relatively small group that was tested might have prevented the detection of these changes.

These results demonstrate the superiority of PET over immunohistochemical and Western blot in detecting early changes in ErbB2 expression. Notably, the benefits gained from imaging receptor changes at an early stage are likely to be even more significant in patients, since tumors in humans usually have a much slower initial growth rate.

After 5 doses of trastuzumab, there was an overall decrease in  $^{18}\text{F}$ -FBEM-HER<sub>2:342</sub> Affibody uptake, and this change was correlated with tumor response. However, there were differences in the responses to trastuzumab among the mice. Tumors showing the greatest decrease in PET signal

shrank, whereas no significant reduction in PET tracer uptake was observed in the nonresponding tumors. We are aware that the arbitrary cutoff values we applied to the analysis of PET images could have some bias, but our data strongly support the statement that the changes in  $^{18}\text{F}$ -FBEM-HER<sub>2:342</sub> Affibody uptake in the range of  $\leq 0.85$  could be a good indicator of treatment outcome. These arbitrary cutoff points could be further validated in future studies. We also confirmed that downregulated ErbB2 expression shown by immunohistochemical staining correlated with the changes in PET signal, thereby validating the results obtained by PET. Our data are also in line with the results reported by McLarty et al., who presented a dramatic decrease in ErbB2 level after 1 dose of trastuzumab as measured by  $^{111}\text{In}$ -diethylenetriaminepentaacetic acid-pertuzumab uptake in mice bearing MDAMB-361 xenografts. Those changes, however, did not correlate with immunohistochemical staining patterns, which showed no apparent alterations in receptor expression. On the other hand, they observed a significant decrease in ErbB2 level as detected by immunohistochemical staining after chronic treatment (3 wk) with trastuzumab (21). Reddy et al. recently reported that a 3-d treatment of SKOV-3 tumor-bearing mice with trastuzumab led to a 42% decrease in tumor uptake of  $^{125}\text{I}$ -C6.5 diabody, which was consistent with a dramatic change in tumor PET signal of  $^{124}\text{I}$ -C6.5 diabody but was not associated with ErbB2 downregulation (22). One possible explanation

for the differences between these groups' observations regarding detection of ErbB2 downregulation by trastuzumab using immunohistochemical staining might be related to the different tumor models used by each group and to specific physiologic parameters, such as vascular permeability and hydrostatic pressure of interstitial fluid. It should also be stressed that the subcutaneous tumor models do not mimic the complex relationship between tumor cells and the stromal microenvironment that is unique to each tissue. Additionally, the variability in detecting ErbB2 downregulation might also be cell line-dependent or, at least in part, hampered by the inability of immunohistochemical staining to sensitively detect subtle changes in receptor expression. Furthermore, it is well known that the antibodies used, as well as the evaluation methods applied in immunohistochemical staining, can produce variable results.

Finally, to understand why certain tumors responded better to trastuzumab than to other treatments, we studied trastuzumab distribution and the vasculature status by checking the number of blood vessels. We found a correlation between bigger PET changes and a higher vessel count, although an elevated number of vessels was found only in the group of animals showing a dramatic decrease in  $^{18}\text{F}$ -FBEM-HER<sub>2:342</sub> Affibody uptake (PET cutoff of  $\leq 0.55$ ). We confirmed that the tumor size was not related to the average vessel count per field and, thus, that we did not simply select tumors that responded to trastuzumab because of better vascularization. Previous studies reported that the number of vessels in a tumor is a useful prognostic marker for treatment response (23). We presume that this increased number of vessels could lead to better trastuzumab delivery, resulting in more sufficient ErbB2 downregulation.

## CONCLUSION

$^{18}\text{F}$ -FBEM-HER<sub>2:342</sub> Affibody-based PET can noninvasively provide specific information about ErbB2 expression and changes in this target receptor, providing a valuable strategy for predicting tumor response to trastuzumab. If verified, such information could allow for monitoring of a patient's immediate response to therapeutic interventions and adjustment of dose and treatment schedules based on the actual receptor status. Such information could also be applied to assess the feasibility of using other ErbB2-targeted therapies to treat tumors that did not respond or acquired resistance to trastuzumab.

## DISCLOSURE STATEMENT

The costs of publication of this article were defrayed in part by the payment of page charges. Therefore, and solely to indicate this fact, this article is hereby marked "advertisement" in accordance with 18 USC section 1734.

## ACKNOWLEDGMENTS

We appreciate the support of Affibody AB and the technical assistance of Monika Kuban and Alesia Holly. The content of this publication does not necessarily reflect

the views or policies of the Department of Health and Human Services, nor does mention of trade names, commercial products, or organizations imply endorsement by the U.S. government. This research was supported in part by the Center for Cancer Research, an Intramural Research Program of the National Cancer Institute; the Imaging Probe Development Center, National Heart, Lung, and Blood Institute; the Breast Cancer Research Stamp Fund, awarded through competitive peer review; the National Cancer Institute under contracts N01-CO-12400 and N01-CO-12401; the NIH Biomedical Research Centre, Oxford; and Breakthrough Breast Cancer through the Holbeck Charitable Trust. No other potential conflict of interest relevant to this article was reported.

## REFERENCES

1. Meric-Bernstam F, Hung MC. Advances in targeting human epidermal growth factor receptor-2 signaling for cancer therapy. *Clin Cancer Res.* 2006;12:6326–6330.
2. Baselga J, Swain SM. Novel anticancer targets: revisiting ERBB2 and discovering ERBB3. *Nat Rev Cancer.* 2009;9:463–475.
3. Tagliabue E, Balsari A, Campiglio M, Pupa SM. HER2 as a target for breast cancer therapy. *Expert Opin Biol Ther.* 2010;10:711–724.
4. Bange J, Zwick E, Ullrich A. Molecular targets for breast cancer therapy and prevention. *Nat Med.* 2001;7:548–552.
5. Scaltriti M, Verma C, Guzman M, et al. Lapatinib, a HER2 tyrosine kinase inhibitor, induces stabilization and accumulation of HER2 and potentiates trastuzumab-dependent cell cytotoxicity. *Oncogene.* 2009;28:803–814.
6. Klapper LN, Waterman H, Sela M, Yarden Y. Tumor-inhibitory antibodies to HER-2/ErbB-2 may act by recruiting c-Cbl and enhancing ubiquitination of HER-2. *Cancer Res.* 2000;60:3384–3388.
7. Gijzen M, King P, Perera T, et al. HER2 phosphorylation is maintained by a PKB negative feedback loop in response to anti-HER2 Herceptin in breast cancer. *PLoS Biol.* 2010;8:e1000563.
8. Clynes RA, Towers TL, Presta LG, Ravetch JV. Inhibitory Fc receptors modulate in vivo cytotoxicity against tumor targets. *Nat Med.* 2000;6:443–446.
9. Barok M, Isola J, Palyi-Krek Z, et al. Trastuzumab causes antibody-dependent cellular cytotoxicity-mediated growth inhibition of submacroscopic JIMT-1 breast cancer xenografts despite intrinsic drug resistance. *Mol Cancer Ther.* 2007;6:2065–2072.
10. Izumi Y, Xu L, di Tomaso E, Fukumura D, Jain RK. Tumour biology: Herceptin acts as an anti-angiogenic cocktail. *Nature.* 2002;416:279–280.
11. Romond EH, Perez EA, Bryant J, et al. Trastuzumab plus adjuvant chemotherapy for operable HER2-positive breast cancer. *N Engl J Med.* 2005;353:1673–1684.
12. Piccart-Gebhart MJ, Procter M, Leyland-Jones B, et al. Trastuzumab after adjuvant chemotherapy in HER2-positive breast cancer. *N Engl J Med.* 2005;353:1659–1672.
13. Cobleigh MA, Vogel CL, Tripathy D, et al. Multinational study of the efficacy and safety of humanized anti-HER2 monoclonal antibody in women who have HER2-overexpressing metastatic breast cancer that has progressed after chemotherapy for metastatic disease. *J Clin Oncol.* 1999;17:2639–2648.
14. Vogel CL, Cobleigh MA, Tripathy D, et al. Efficacy and safety of trastuzumab as a single agent in first-line treatment of HER2-overexpressing metastatic breast cancer. *J Clin Oncol.* 2002;20:719–726.
15. Ghosh R, Narasanna A, Wang SE, et al. Trastuzumab has preferential activity against breast cancers driven by HER2 homodimers. *Cancer Res.* 2011;71:1871–1882.
16. Dijkers EC, Oude Munnink TH, Kosterink JG, et al. Biodistribution of  $^{89}\text{Zr}$ -trastuzumab and PET imaging of HER2-positive lesions in patients with metastatic breast cancer. *Clin Pharmacol Ther.* 2010;87:586–592.
17. Perik PJ, Lub-De Hooij MN, Gietema JA, et al. Indium-111-labeled trastuzumab scintigraphy in patients with human epidermal growth factor receptor 2-positive metastatic breast cancer. *J Clin Oncol.* 2006;24:2276–2282.



18. Eigenbrot C, Ultsch M, Dubnovitsky A, Abrahmsen L, Hard T. Structural basis for high-affinity HER2 receptor binding by an engineered protein. *Proc Natl Acad Sci USA*. 2010;107:15039–15044.
19. Kramer-Marek G, Kiesewetter DO, Capala J. Changes in HER2 expression in breast cancer xenografts after therapy can be quantified using PET and F-18-labeled Affibody molecules. *J Nucl Med*. 2009;50:1131–1139.
20. Kiesewetter DO, Kramer-Marek G, Ma Y, Capala J. Radiolabeling of HER2-specific Affibody (R) molecule with F-18. *J Fluor Chem*. 2008;129:799–805.
21. McLarty K, Cornelissen B, Scollard DA, Done SJ, Chun K, Reilly RM. Associations between the uptake of <sup>111</sup>In-DTPA-trastuzumab, HER2 density and response to trastuzumab (Herceptin) in athymic mice bearing subcutaneous human tumour xenografts. *Eur J Nucl Med Mol Imaging*. 2009;36:81–93.
22. Reddy S, Shaller CC, Doss M, et al. Evaluation of the anti-HER2 C6.5 diabody as a PET radiotracer to monitor HER2 status and predict response to trastuzumab treatment. *Clin Cancer Res*. 2011;17:1509–1520.
23. Hironaka S, Hasebe T, Kamijo T, et al. Biopsy specimen microvessel density is a useful prognostic marker in patients with T2-4M0 esophageal cancer treated with chemoradiotherapy. *Clin Cancer Res*. 2002;8:124–130.